Droplet impacts of non-Newtonian fluids for bioengineering applications

A. S. Moita[1], D. Hermann[1] and A. L. N. Moreira[1]

1: Laboratory of Thermofluids, Combustion and Energy Systems, IN+, Dep. Mechanical Eng., Instituto Superior Técnico, Univ. Técnica de Lisboa, Portugal

Abstract

The present paper is part of a broader project addressing the experimental and theoretical description of the dynamic behaviour of non-Newtonian droplets impacting on cold and heated surfaces. Main focus is put in the description of power-law fluids, particularly shear-thinning, for bioengineering applications. In this context, a parametric study is performed to evaluate the post-impact behaviour of Newtonian and shear-thinning droplets, within a wide range of impact conditions (28<We<448). Several models devised for Newtonian droplet impacts are adapted and their accuracy is compared for the shear-thinning. The results evidence the increase of the consistency coefficient *K* with the mass concentration of the shear-thinning element and stress the dominant role of this parameter in describing droplet's spreading and receding motions. This effect can be well described by the Cross constitutive model and is significantly enhanced when the surface is heated. The Cross model was successfully used to determine the equivalent dimensionless numbers that were required to adapt the energy conservation approach, to estimate the spreading diameter of the shear-thinning droplets. Additional research is however required to fully integrate the dependence of the viscosity of these complex fluids with the temperature.

Introduction

Unlike Newtonian fluids, for which the stress tensor is a linear function of the velocity gradient and therefore the viscosity remains constant regardless of the shear rate, in non-Newtonian (or complex) fluids, the stress tensor is a generic function of the velocity gradient and of its derivatives [1]. When a droplet impacts a solid surface, large spatial and temporal gradients are observed, so the dynamic behaviour of a non-Newtonian droplet can be significantly different from that of a Newtonian one. Despite most of the studies on droplet impacts focus on Newtonian fluids, many applications deal in fact with non-Newtonian liquids. There are different classes on non-Newtonian fluids, namely power-law-fluids, viscoelastic and yield-stress (or Bingham plastic) [1], whose viscosity-shear rate dependence is governed by different constitutive models. Although significant breakthrough has been achieved to experimentally describe the spreading and the rebound behaviour of viscoelastic, yield-stress and shear-thinning fluids (*e.g.* [2-6]), the results are sometimes contradicting as the physical description of the phenomena is mostly based on a pure empirical description. In fact, several constitutive models are based on empirically fitting parameters, but the effect of each parameter is not understood, either is their relation with the composition of the fluids. For instance, the simplest non-Newtonian fluids are probably the so-called power-law-fluids. For these, the viscosity is not constant, but is a polynomial function of the shear velocity gradient, described as:

$$\tau = K\left(\frac{\partial u}{\partial y}\right)^n \tag{1}$$

being τ the shear stress and $\partial u/\partial y$ the velocity gradient. Here, *K* is the consistency coefficient and *n* the power law index. For $n<1$, one obtain the so-called shear-thinning (or pseudoplastic) fluids, while for $n>1$ one has the shear (thickening) or dilatant fluids. For $n=0$, equation (1) describes the behaviour of Newtonian fluids, so that the consistency coefficient coincides with the Newtonian viscosity. Recently, German and Bertola [7] have discussed on the role of *K* and of *n* in the spreading behaviour reporting a non-intuitive result: as the concentration of a shear thinning component increases, *n* increases, so one should expect lower spreading diameters, since there should be a larger viscosity at high velocity gradients (at the beginning of spreading), which would promote energy dissipation. However, the opposite trend is observed. The *n* and *K* parameters cannot be independently observed because changing the mass concentration also affects *K* in the opposite trend of *n*. So, larger concentration leads to thicker fluids (large "zero" viscosity) but more shear-thinning (low "infinite" viscosity). This variation of the viscosity between a minimum and a maximum, for low and high shear rates is quantitatively described by a number of constitutive models [8, 9], whose validation and fitting are still dependent from appropriate experimental data. Additionally, it is not clear yet how the constitutive models

change with different parameters such as the liquid/surface temperature, despite the fact that, for many of the aforementioned applications, the surface temperature is an important variable.

Since many coating and painting solutions are shear-thinning, describing accurately the post-impinging behaviour and particularly, being able to accurately predict the spreading and receding diameters of this class of fluids is of major importance. Another particular reason to focus on this class of non-Newtonian fluids is in the creation of new interfaces and biomaterials, using the so-called cell printing method. Here, the cells or organic preparations are printed on demand on "bio-papers", so that they can grow with customized direction/organization (*e.g.* [10]). Only recently the deposition process was modelled by Bioengineers based on impacts of Newtonian droplets (*e.g.* [11]), in order to try to predict the desired cell disposition. On the other hand, when living cells are used, they are extremely sensitive to shear stress, so that the velocity rates inside the droplet during the spreading must be accurately quantified. Ultimately, the appropriate impact conditions are chosen to assure the desired deposition process while keeping the cells viable. Many of these preparations also have shear-thinning characteristics, so, also here, description of the post impingement spreading and receding motions is of vital importance.

In line with this, the present work addresses the description of the effect of the mixture concentration on the parameters governing the constitutive models of shear-thinning fluids. These are then used to derive equivalent dimensionless numbers, which are required to devise the spreading models equivalent to those available for Newtonian drops, as in [12, 13]. A parametric study is performed to evaluate the post-impact behaviour of Newtonian and shear-thinning droplets, within a wide range of impact conditions ($28<We<448$). Several models devised for Newtonian droplet impacts are adapted and their accuracy is compared for the shear-thinning liquids, as a function of the impact conditions, mixture composition and surface temperature. Surface topography and wettability will be explored as a way to play with the parcel of the dissipated energy.

Experimental Procedure

The experiments encompass the impact of droplets within a wide range of diameters ($80\mu m<D_0<3.3mm$) impacting on solid and dry surfaces, surfaces with velocities U_0 ranging from 0.88 to 7m/s. For this paper, only the results obtained with the millimetric droplets are discussed.

The surfaces are accommodated on a copper base in which a 264 W cartridge heater is inserted and are heated from room temperatures up to 140ºC. Surface temperature of the targets is acquired using fast response type K thermocouples "Medtherm". The thermocouples are 3mm apart, taking from the reference the thermocouple that is placed in the center of the droplet impact region (r=0mm). They are aligned with the top of the surface where the impact occurs. Another embedded thermocouple is used to control the cartridge heaters, using a PMA KS20-I controller. Care is taken to assure that the surface is dry and recovers the initial temperature before the impact of the droplet. The liquid is kept at the droplet generator at room temperature and atmospheric pressure. Ambient temperature and relative humidity were measured through the experiments to ensure that their variation did not produce relevant changes in the results.

The signal of the thermocouples is sampled with a National Instruments DAQ board associated with a BNC2120 and amplified with a gain of 300 before processing. Different acquisition frequencies were used to characterize the temporal variation of the instantaneous temperature. Hence, to capture the entire variation along droplet deformation process, a relatively low frequency must be used (of the order of 2Hz). Then to refine the measures to particular instants a larger frequency was considered, of the order of 10kHz.

Droplet impacts are recorded using a high-speed camera (Phantom v4.2 from Vision Research Inc., with 512x512pixels@2100fps and a maximum frame rate of 90kfps). To record the impact history of the millimetric droplets, the frame rate was set to 2200fps. For the micrometric droplet streams the frame rate was increased up to 6300 fps (208 x 400 pixels). For the set-up used here, the resolution is 25pixel/mm.

The behaviour of non-Newtonian liquid droplets is compared with that of water and water-glycerine mixtures. The non-Newtonian liquid drops are made of different water+xanthan gum (G1253, Sigma-Aldrich) solutions at levels of 0.05%, 0.1%, 0.2% and 0.35% wt%. Shear viscosities were measured using capillary viscometer and rotational rheometer. Specific mass and surface tension of all the xanthan gum solutions are very close of those of water, as depicted in Table 1. Although, different concentrations, namely 0.05, 0.1, 0.15, 0.20, 0.25, 0.30 and 0.35wt% are being tested, due to paper length constrains, most of the results discussed here were obtained for the extreme limits of xanthan mass fraction, 0.05% and 0.35%, which are presented in the table.

Table 1. Thermophysical properties of the working liquids taken at 20ºC.

Liquid	Specific mass ρ [kg/m3]	Surface tension σ_{lv} [mN/m]	Dynamic viscosity η_0 [Pa.s]	Dynamic viscosity η_∞ [Pa.s]

Water	998	72.75	$8.9x10^{-4}$	$8.9x10^{-4}$
X0.05 (Xanthan gum 0.05wt%)	999	73.0	0.12	$1.2x10^{-3}$
X0.05 (Xanthan gum 0.35wt%)	999	72.95	12.5	$2.0x10^{-3}$

Characterization of the test surfaces

The surfaces used here are made from a silicon wafer and are micro-patterned using square structural, with side size *l* and height *h*. The pillars are apart within a distance λ_R, as defined in Figure 1. The patterns are printed on the silicon wafer by lithography and processed by plasma etching. To reach higher pillars, the wafer surfaces were coated with aluminum, before the lithography. So, besides plasma etching, wet chemical etching is required for the aluminum coating. The micro-patterns are controlled to have known, precise values, using a profilemeter, with a measurement precision of ±100Angstroms. An example of a roughness profile is depicted in Figure 1. Finally, the surfaces are checked by SEM/EDS analysis. Heterogeneity of the patterns was found to be lower than 3%. The wettability of the surfaces was also characterized, based on the static and dynamic contact angles, measured at room temperatures using an optical tensiometer THETA from Attesion.

An average value is considered for each pair liquid-surface which is determined from at least eight measurements taken at different regions of the surface. The time evolution of the average contact angles is obtained by curve fitting and the final values are determined by extrapolation. The detailed measurement procedure has been described in previous works (*e.g.* Moita and Moreira [14]).

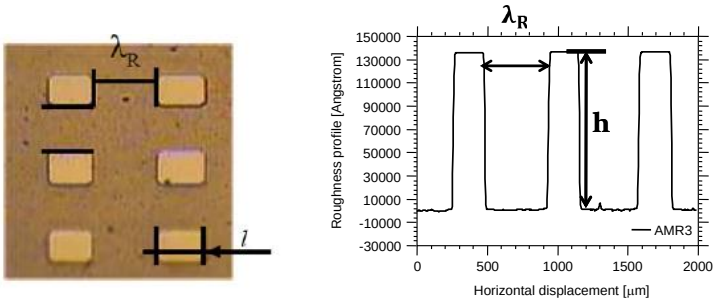

a) **b)**

Figure 1. a) Detail of a micro-structured surface, showing the definition of the dimensions *a*, *h*, and λ_R characterizing its topography. **b)** Sample 1-D roughness profile of the surface.

Results and Discussion

The qualitative analysis of droplet impact taken from high-speed visualization of its post-impingement morphology shows that the dynamic behaviour of the shear-thinning droplets dos not depict any particular morphology, when compared to that of Newtonian droplets, but the impact outcomes can be significantly different. Hence, a fast expansion of the lamella is observed for the xanthan mixture with 0.35 wt%, which is followed by a slow spreading with a moderately low expansion diameter. Compared with water, the fast expansion, which occurs right after the impact is related to the shear thinning effect, but then, as the shear rate quickly decreases, as the lamella approaches its maximum diameter, the zero viscosity tends to increase, thus limiting the value of the spreading diameter. This is not very clear in the illustrative images shown in Figure 2, but is obvious in the plots in Figure 3, which depict the temporal evolution of the spreading ratio $\beta=d(t)/D_0$, where d(t) is the spreading diameter of the lamella and D_0 is the initial droplet diameter. A similar trend is observed for higher impact velocities, since although the shear rates at the beginning of the expansion of the lamella are higher, thus decreasing the viscosity, the dissipation associated to these large velocity gradients is actually larger. Then, the viscosity tends to increase at the end of the expansion of the lamella. Consequently, the receding motion is very slow for these high concentrations of xanthan, so the spreading and equilibrium diameters remain larger than those of water, both for cold and heated surfaces, even though its zero shear rate viscosity is significantly higher than that of water.

A different trend is nevertheless observed for the xanthan mixture with the lowest concentration (0.05wt%): in this case, the spreading behaviour is similar to that observed for the 0.35wt% concentration. However, very fast recoil is instead observed for the liquid with the smallest concentration, which can be even slightly faster

than that observed for water droplets. This is particularly evident at the highest impact velocity and when the surface is heated. Indeed, augmenting the surface temperature seems to stress this fast recoiling motion for the xanthan mixture with 0.05wt%, which actually results in a partial rebound for the impact at the highest velocity (Figure 3d). Similar rebound phenomenon is reported in [13], for impacts onto hydrophobic surfaces, for which the energy dissipation is lower. Hence, one may speculate that the temperature is acting on the *K* and *n* factors in a way that, overall the entire spreading and receding process, a smaller parcel of the surface energy is dissipated.

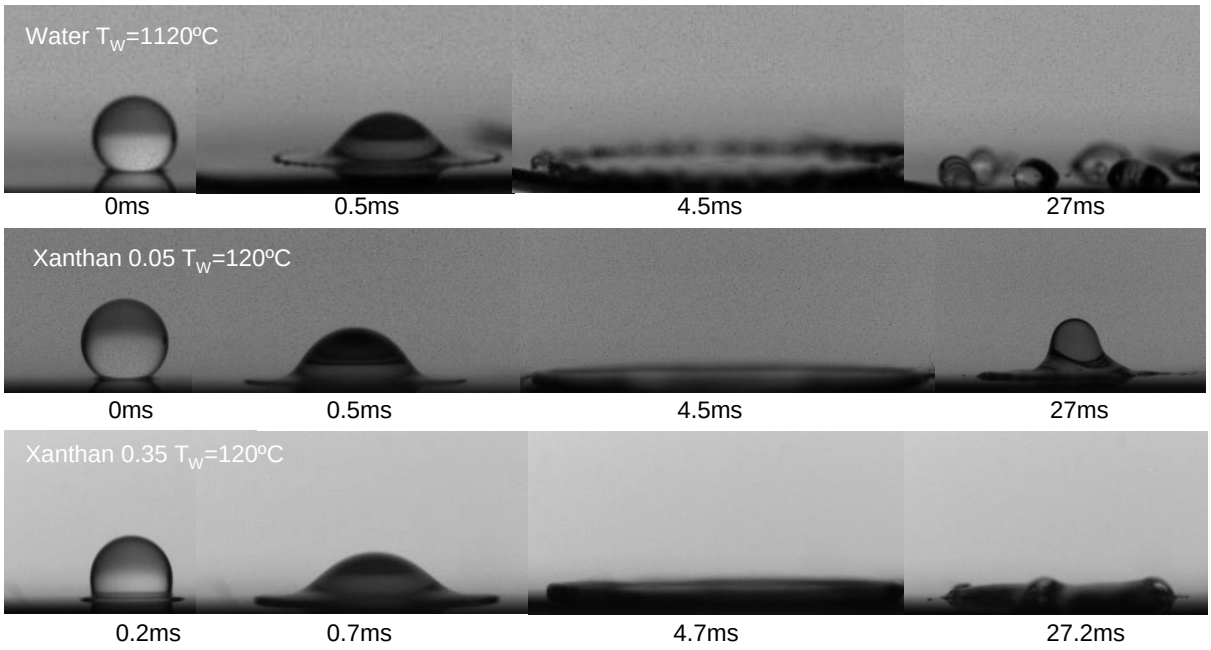

Figure 2. Impact of water and water-xanthan gum mixtures impacting a smooth silicon wafer, heated at T_W=120ºC. For all the droplets D_0=3.2mm and U_0=3.2m/s.

A wider view of how the maximum spreading ratio are varying, for different wt% of xanthan gum and for various surface temperatures, as a function of the impact velocity (quantified here as the Weber number) is further presented in Figure 4. Our results are depicted here together with those reported by [13] for comparative proposes and to allow a more general analysis, covering a wider range of data.

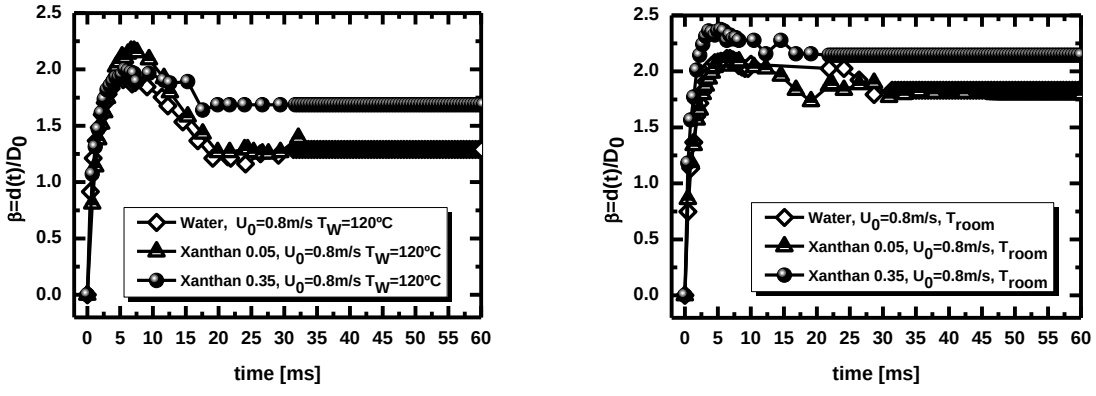

a) **b)**

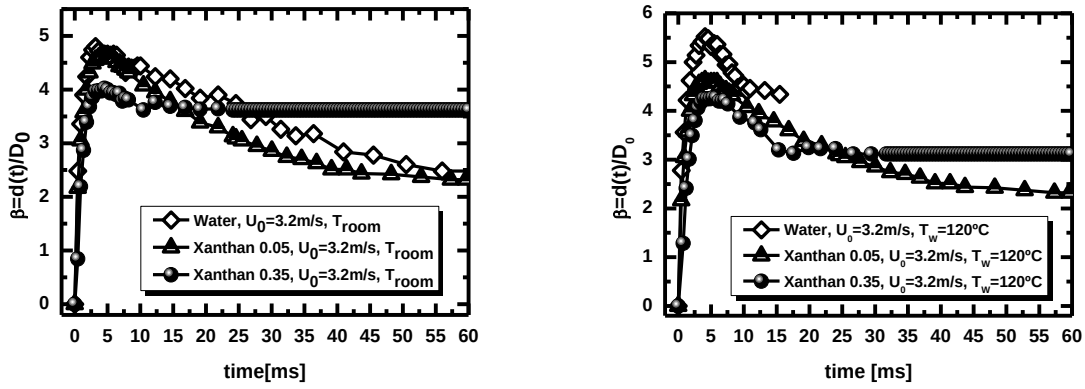

c) **d)**

Figure 3. Spreading ratio for water and xanthan gum mixtures impacting onto a smooth silicon surface at: a)U_0=0.8m/s, room temperature; b) U_0=0.8m/s, surface temperature T_W=120ºC; c)U_0=3.2m/s, room temperature; d) U_0=3.2m/s, surface temperature T_W=120ºC.

The results depicted here, can be explained as follows. As the mass fraction of the shear-thinning element increases, *K* in equation (1) increases, while *n* decreases [7]. According to the behaviour described above, *K* seems to play the dominant role, and represents the maximum viscosity that the fluid may exhibit. These findings are in agreement with those reported in [7]. The fact that the surface temperature enhances this behaviour is not yet clear and deserves further investigation. This behaviour should be carefully taken into account for applications dealing with heat transfer such as for cooling purposes. Lower concentrations of the shear thinning element actually result in expanding spreading diameters, for higher temperatures, but also lead to fast recoiling motion, which can significantly reduce the contact time and contact area of the liquid over the surface to cool, within a temporal range which is still relevant for the heat transfer characteristic times. A way to compensate this enhanced recoiling motion can be by playing with the surface wettability, at the expense of altering its topography. At this stage it is still yet to soon to withdrawn any conclusion, but preliminary results, suggest that an average well controlled spreading diameter can be achieved for non-Newtonian droplets, impacting onto micro-patterned surfaces, which are actually quite similar to those obtained for Newtonian droplets, as previously reported in [15]. Although speculative, this result is contrasting with previous findings, *e.g.* [7] who report a minor role of the surface wettability on the dynamic behaviour of shear-thinning droplets, and can be explained by the fact that in the present work the wettability is mainly varied at the expense of changing the surface topography, not only affecting the usual energy dissipation occurring at the contact line, due to contact angle hysteresis, but is also possibly influencing the viscous dissipation.

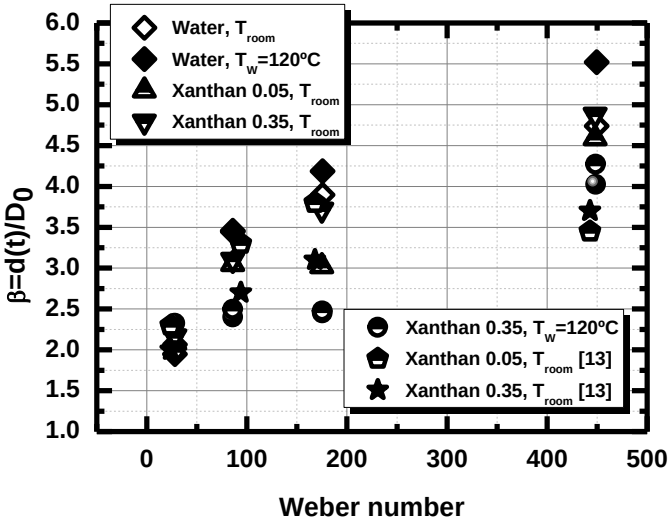

Figure 4. Spreading ratio as a function of the impact Weber number for different wt% of the Xanthan gum, for diverse surface temperatures.

Regarding to the prediction of the spreading diameter, the variation of the viscosity between zero and infinite shear during the entire deformation process is well related to the Cross model: $\frac{\eta_{eff}-\eta_\infty}{\eta_0-\eta_\infty}=\frac{1}{1+\left(k.C\frac{3\beta_{max}^2U_0}{2D_0}\right)^m}$. At this stage of the work, a semi-empirical approach is still required to be followed to determine the parameters *k*, *C* and *m*, as in [14]. Here, the shear rate is scaled, following a similar approach to that of [14], based on mass conservation principles. This procedure allows determining equivalent viscosities which were used to compute equivalent Ohnesorge $Oh_{eff}=\frac{\eta_{eff}}{(\rho D_0\sigma_{lv})^{1/2}}$ and Reynolds $Re_{eff}=\frac{\rho U_0 D_0}{\eta_{eff}}$ numbers, which in turn are used to evaluate the equivalent model following that of Scheller and Bousfield [16], in the general form: $\beta_{max,predicted}=C_1(Re_{eff}^2\,Oh)^n$ .The results show an acceptable good agreement between the experimental data and the predicted values, although the enhanced effect of the surface temperature is not completely well captured. Additionally, a more complex scaling of the shear rate is required, to be consistent with the non-uniform thickness of the rim, as suggested for instance by Roisman [17].

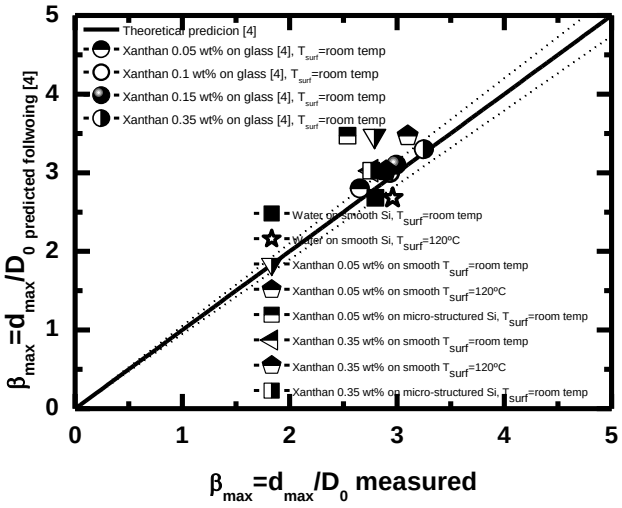

Figure 5. Comparison between our experimental results and the predicted values of the maximum spreading diameter made dimensionless by droplet initial diameter $\beta_{max,predicted}$, following the approach of [14].

Final Remarks

The present paper is part of a broader project addressing the experimental and theoretical description of the dynamic behaviour of non-Newtonian droplets impacting on cold and heated surfaces. Main focus is put in the description of power-law fluids, particularly shear-thinning, for bioengineering applications. In this context, a parametric study is performed to evaluate the post-impact behaviour of Newtonian and shear-thinning droplets, within a wide range of impact conditions (28<We<448). Several models devised for Newtonian droplet impacts are adapted and their accuracy is compared for the shear-thinning liquids. The results evidence the increase of the consistency coefficient *K* with the mass concentration of the shear-thinning element and stress the dominant role of this parameter in describing droplet's spreading and receding motions. This effect can be well described by the Cross constitutive model. Hence, larger mass concentrations of the shear thinning element lead to smaller viscosities at high shear rates and larger viscosities occur at low shear rates. Consequently, significant energy dissipation occurs at the earliest spreading stages, when the shear rates are higher, for the largest mass concentration drops. On the other hand, larger viscosity is obtained as the spreading lamella reaches the maximum expanding diameter and decelerates. Therefore the lowest maximum spreading diameters generally occur for the largest mass concentrations of the shear-thinning element, for which the receding motion is almost inexistent. This behaviour contrasts with the large and fast spreading, recoiling and even rebound, which are observed for the impact of the droplets with the lowest concentration of the shear-thinning element. This effect is significantly enhanced when the surface is heated.

The Cross model was successfully used to determine the equivalent dimensionless numbers that were

necessary, in order to adapt the energy conservation approach, to estimate the spreading diameter of the shear-thinning droplets. Additional research is however required to fully integrate the dependence of the viscosity of these complex fluids with the temperature.

Acknowledgements

The authors are grateful to Fundação para a Ciência e a Tecnologia (FCT) for partially financing the research under the framework of the project PTDC/EME-MFE/109933/2009 and for supporting A.S. Moita with a Fellowship (Ref: SFRH/BPD/63788/2009).

References

[1] V. Bertola, M. Marengo, Koninklijke Brill NV, Leiden (2012).
[2] R. Crooks, D.V. Boeger., *J. Rheol*., 44:973-996 (2000).
[3] A. Rozhkov, B. Prunet-Foch, M. Vignes-Adler, *Phys. Fluids*, 15:2006-2019 (2003).
[4] V. Bertola, *Exp. Fluids*, 37:653-664 (2004).
[5] D. Bartolo, A. Boudaoud, G. Narcy, D. Bonn, *Phys. Rev. Lett.*, 99:174502 (2007).
[6] M. Smith, V. Bertola, in: *Proc. 23rd Annual Conf. Liquid Atom. Spray Syst. – ILASS Europe-2010*, p.124 (2010).
[7] G. German, V. Bertola, *J. Phys. Condens. Matter*, 21:16pp (2009).
[8] M. M. Cross, *J. Coll. Sci.*, 20:417-437 (1965).
[9] P. J. Carreau, *PhD Thesis*, University of Wisconsis, Madison,USA (1968).
[10] S. Tasoglu, G. Kaynak, A. J. Szeri, U. Demirci, M. Muradoglu, *Phys. Fluids*, 22:082013 (2010).
[11] T. Xu, J. Jin, C. Gregory, J. J. Hickman, T. Boland, *Biomaterials*, 26:93-99 (2008).
[12] S. M. An, S. Y. Lee, *Exp. Thermal Fluid Sci.*, 37:37-45 (2012).
[13] S. M. An, S. Y. Lee, *Exp. Thermal Fluid Sci.*, 38:140-148 (2012).
[14] A. S. Moita, A. L. N. Moreira, *Exp. Fluids*, 52:679:695 (2012).
[15] A. S. Moita, A. L. N. Moreira, in: *Proc. 12th Triennial Int. Conf. Liquid Atom. Spray Syst. – ICLASS 2012*.
[16] B. L. Scheller, D.W. Bousfield, *AIChe J.*, 41:1357-1365 (1995).
[17] I.V. Roisman, *Phys. Fluids*, 21:052104 (2009).